Lifshitz-Safran Coarsening Dynamics in a 2D Hexagonal System

Leopoldo R. Gómez and Enrique M. Vallés

Planta Piloto de Ingeniería Química (UNS-CONICET), Camino La Carrindanga, KM 7, 8000 Bahía Blanca, Argentina

Daniel A. Vega*

Department of Physics, Universidad Nacional del Sur, CONICET, Avenida L. N. Além 1253, 8000 Bahía Blanca, Argentina

The coarsening process in a two-dimensional hexagonal system in the region close to both spinodal and order-order transitions was investigated through the Cahn-Hilliard model. We found a distinctive region of the phase diagram where the pinning of dislocations plays only a minor role and the dynamics is led by the triple points. In this region, we found configurations of domains with the same features as those proposed by Lifshitz. As a consequence, different correlation lengths grow logarithmically in time, in good agreement with the predictions of coarsening at low temperatures proposed by Safran.

The mechanism of coarsening in a two-dimensional system undergoing phase separation following a quench from the high temperature phase to the ordered phase has been the subject of intense investigations for more than three decades [1,2]. Except in certain exceptional circumstances, it has been clearly shown through numerous studies that different systems show a coarsening process satisfying scaling at long times [1]. In this case, the dynamics can be characterized by a simple length scale $\xi(t)$ that grows in time t as a power law ($\xi \sim t^q$) [1,3]. This feature has also been observed experimentally in thin films of block copolymers in the smectic phase [4,5]. In this case, it was shown that the orientational correlation length grows in time as $\xi_2 \sim t^{1/4}$ and that the dynamics is led by the annihilation of multipoles of disclinations. On the other hand, it has recently been found through simulations [6] and experiments [7] that, in sphere-forming block copolymer thin films, the orientational and translational correlation lengths grow according to different kinetic exponents. The difference in kinetic exponents has been attributed to a preferential annihilation of dislocations located along small angle grain boundaries [6].

In the 1960s, Lifshitz predicted the possibility of formation of a stable lattice of domains on a system with p-fold degenerate equilibrium states. According to Lifshitz, this lattice should emerge during the coarsening process due to the dynamic frustration to reach equilibrium [8]. Although this grain structure would not minimize the total free energy of the system, it was shown that it could be kinetically stable. As a consequence of the relaxation driven by the curvature of grain boundaries, bounded regions where three grains meet [triple points (TP)] can become pinned to their positions, slowing down the dynamics. Once the system becomes trapped into this dynamically stable state, the only path to induce further coarsening is through fluctuations or driving forces large enough to unlock the system from the local traps. The first step to introducing Lifshitz's ideas in the coarsening process quantitatively was made by Safran [9]. It was found

that the domains grow according to a power law in time for $p < d + 1$ (d is the spacial dimensionality) but logarithmically in time in the case $p \geq d + 1$.

Although a few systems have been found where the growth of the correlation length is logarithmic [10], to the best of our knowledge, there are no systems clearly verifying the Lifshitz-Safran predictions at present.

The dynamics of phase separation for a diblock copolymer can be described by the following time-dependent Ginzburg-Landau equation for a conserved order parameter (Cahn-Hillard model) [11]:

$$\frac{\partial \psi}{\partial t} = M \nabla^2 \left\{ \frac{\delta F}{\delta \psi} \right\}. \tag{1}$$

In this equation, the order parameter ψ is defined in terms of the local density of each block in the block copolymer, M is a phenomenological mobility coefficient, and F is the mean-field free energy functional for a diblock copolymer [11]:

$$F = \int d\mathbf{r}^3 \left[U(\psi) + \frac{D}{2}(\nabla \psi)^2 \right]$$
$$- \frac{b}{2} \iint d\mathbf{r}^3 d\mathbf{r}'^3 G(\mathbf{r} - \mathbf{r}') \psi(\mathbf{r}) \psi(\mathbf{r}'). \tag{2}$$

Here $G(\mathbf{r})$ is a solution of $\nabla^2 G(\mathbf{r}) = -\delta(\mathbf{r})$, and $U(\psi) = \frac{1}{2}[-\tau + a(1 - 2f)^2]\psi^2 + \frac{1}{3}\nu\psi^3 + \frac{1}{4}\lambda\psi^4$. The parameters a, ν, b, and λ are related to the vertex functions derived by Leibler [12]. The parameter τ depends linearly on the Flory-Huggins parameter χ and provides a measurement of the depth of quench. f is the block copolymer asymmetry, and D is a parameter related to the segment length [11].

Equation (1) leads to spinodal decomposition for $\tau > \tau_s = 2\sqrt{bD} + a(1 - 2f)^2$ and to an order-order transition (hexagonal-smectic transition) for $f = f_c = 1/2$ ($\tau = 2\sqrt{bD}$).

In this work, we solve Eq. (1) in the region near both the order-order and spinodal transitions ($\tau \gtrsim \tau_s$, $f \lesssim f_c$) for a

2D system with hexagonal symmetry containing $\sim 2.5 \times 10^4$ disks (see Ref. [6] for details). In Fig. 1, we show typical pattern configurations at a given depth of quench ($\tau_r = 10^{-4}$, where $\tau_r = \tau/\tau_s - 1$) and different coarsening times. In this figure, we show the results corresponding to two different values of f_r ($f_r = 1 - f/f_c$). Figures at the top correspond to $f_r = 0.03$ and at the bottom to a region closer to the order-order transition ($f_r = 0.01$). By comparing the figures with different block copolymer asymmetries, we can observe qualitatively the increase in the interface thickness as the order-order transition is approached ($f \rightarrow f_c$). Note also the presence of hexagonal cells at grain boundaries. The right panels in Fig. 1 show color maps of the orientational field for the same images at the center of this figure. The color key (shown at rightmost panel of the figure) indicates the orientational field over the range $[0, \pi/3]$, as appropriate for a sixfold symmetric structure. Through the color map, regions with similar orientation can be easily identified. The local orientation is determined in real space by a Delaunay triangulation [7].

To determine the features of the interface quantitatively, we employ the model proposed by Goveas and Milner to study the lamellar-cylindrical transition in weakly segregated diblock copolymer melts [13]. Here we consider a two parameter family of ordered phases generated by a linear superposition of two hexagonal patterns rotated in an angle α. Then we construct an order parameter: $\Psi(\mathbf{r}) = (\phi/\sqrt{3}) \sum \{\exp(i\mathbf{q}_1 \cdot \mathbf{r}) + \text{c.c.}\} + (\varphi/\sqrt{3}) \times \sum \{\exp(i\mathbf{q}_2 \cdot \mathbf{r}) + \text{c.c.}\}$. The sets $\{\mathbf{q}_1\}$ and $\{\mathbf{q}_2\}$ contain the wave vectors corresponding to the two hexagonal patterns misoriented by the desired angle. By expanding the free energy up to fourth order in the above amplitudes, we found that the local free energy can be expressed as:

$$\frac{\tilde{F}N}{kT} = [-\tau + a(1 - 2f)^2](\phi^2 + \varphi^2) + \frac{4}{3\sqrt{3}} \nu(1 - 2f)$$
$$\times (\phi^3 + \varphi^3) + 2\lambda(\phi^4 + \varphi^4) + 6\lambda\phi^2\varphi^2.$$

Note that this result is independent of the angle α. As in the lamellar-cylindrical case, here we found that close to coexistence the free energy can be parametrized with a unique amplitude along the path of steepest descent and can be approximated by a symmetric quartic $\tilde{F}(\phi) - \tilde{F}(\phi_{\min}) \sim [1 - (2\phi/\phi_{\min} - 1)^2]^2$. The next step takes into consideration the following dynamical equations for the evolution of the superposed patterns: $\Gamma \frac{d\phi}{dt} = -\frac{\delta H}{\delta\phi}$ and $\Gamma \frac{d\varphi}{dt} = -\frac{\delta H}{\delta\varphi}$. Here Γ is a drag coefficient and the Hamiltonian H contains the free energy cost to create interfaces and the local term $\tilde{F}(\phi, \varphi)$, i.e., $H \sim \int d^3 r[a_0^2(\nabla\phi)^2 + a_0^2(\nabla\varphi)^2 + \tilde{F}(\phi, \varphi)]$, where a_0 represents a monomeric length. Using these equations, it can be shown that at coexistence the shape of the interfaces presents the usual hyperbolic tangent profiles and that the thickness of the interfaces diverges at the critical point as $1/f_r$. An equivalent result for the thickness of the interface was found in hexagonal patterns of a Swift-Hohenberg model for Rayleigh-Benard convection [14].

As a consequence of the superposition of misoriented grains, the interface is decorated with hexagonal cells with sizes which depend on the misorientation. This feature is clearly observed in Fig. 1(c), where misorientational-dependent cell sizes are formed. These moiré patterns are obtained by the linear superposition of two hexagonal patterns rotated by a certain angle. For grains with a disorientation α, the cell size must grow as α^{-1}.

Through the Delaunay triangulation, it is also possible to determine the topological defects; in our case, we analyze the time evolution of translational (dislocations) and orientational (disclinations) defects [7]. In the color maps in Fig. 1, we have included the topological defects. Since the disclination charge is strongly modified by the presence of dislocation lines [15], these defects introduce only small perturbations in the orientational field.

Similarly to hard crystalline solids, here we found that grain boundaries are well described as an array of disloca-
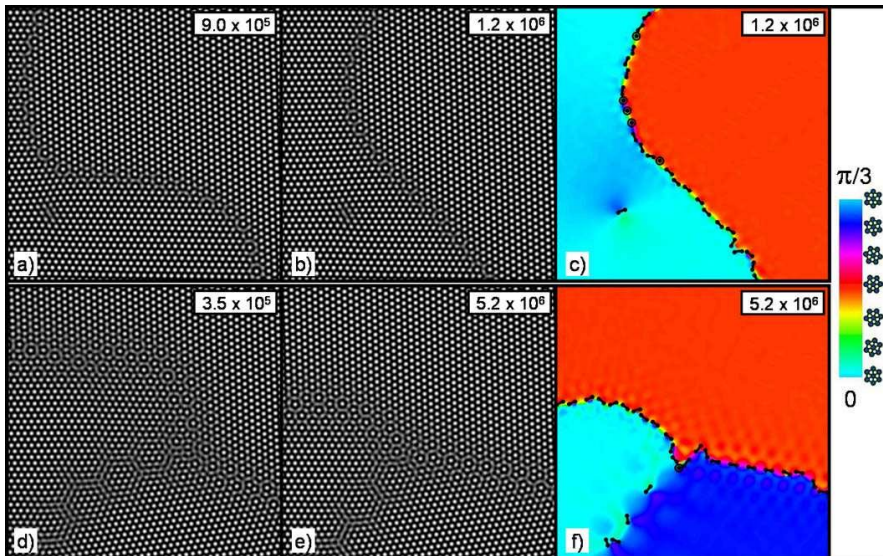

FIG. 1 (color online). Patterns and orientational maps obtained at different values of f_r and simulation times (indicated in the figure). The patterns in the left panel correspond to short times and in the middle to long times. In the orientational maps, dislocations have been indicated with a black line and disclinations with an open circle. The rightmost side of the figure shows the gray scale (color scale) used to indicate local orientation.

tions separated by an average distance of the order a/α [6], where a is the interdisk distance (lattice constant). Then the size of the cells shown in Fig. 1 and the average distance between dislocations are commensurate. This feature can be observed in Fig. 1 [16].

In different systems with hexagonal symmetry, it has been found that the coarsening freezes at deep quenches ($\tau_r \gg 1$) [6,14]. In this case, the system becomes trapped into a metastable state and it is unable to reach equilibrium. By taking into account nonadiabatic correction to the evolution equations, Boyer and Viñals [14] have shown that this is due to the presence of pinning forces. These pinning forces were shown to be the analogs of the Pierls forces acting on dislocations in crystalline solids.

Figures 1(a) and 1(b) show the results of the simulation for two different stages of the coarsening process. One immediately notices the grain boundary motion and the relaxation of curvature in Fig. 1(b) as compared with Fig. 1(a). Although present, the pinning forces acting on the dislocations are clearly defeated by the line tension along the grain boundary. If driven purely by curvature, the dynamics is expected to be led by a power law. However, by the reasons discussed below, here the dynamics becomes slower.

To determine the time evolution of the degree of ordering in the system, we compute different correlation lengths. The orientational correlation length ξ_6 can be determined by approximating the circularly averaged orientational correlation function $g_6(r)$ with a single exponential: $g_6(r) \sim \exp(-r/\xi_6)$. Here $g_6(r)$ is defined as $g_6(r) = \langle \exp[6i(\theta(r) - \theta(r'))]\rangle$, where θ represents the local bond orientation (see Ref. [7] for details). Figures 1(c) and 1(f) show the color maps with the local orientation θ of the lattice. Note the orientational distortions introduced by dislocations.

A characteristic correlation length ξ_s can be determined through the full width at half maximum of the main peak of the scattering function $S(k) = \langle \tilde{\psi}(\mathbf{k})\tilde{\psi}(\mathbf{k})^* \rangle$. We also analyze the correlation lengths defined through the density of dislocations ρ_{ds} and the density of disclinations ρ_{dl}. A correlation length associated to disclinations can be defined as $\xi_{dl}(t) \sim \rho_{dl}(t)^{-1/2}$ [7]. Here we found that most of the disclinations are bound to TP. Differently from the disclinations, the dislocations are not randomly distributed, but they appear to be decorating the grain boundaries. Then a characteristic grain size defined by a dislocation array can be defined as $\xi_{ds}(t) \sim \rho_{ds}(t)^{-1}$ [6].

Figure 2 shows the temporal evolution of the various correlation lengths studied here. Differently from previous works on block copolymers where the correlation lengths grow according to a power law [4,6,7], here we found a logarithmic dependence in time. This feature is clearly observed in Fig. 2 through the linear fits to the different correlation lengths.

In Fig. 3, we show the process of coarsening as viewed through the orientational maps. In the time sequence of this figure, it is possible to observe the motion and annihilation of TP (triangles). During this process, however, a
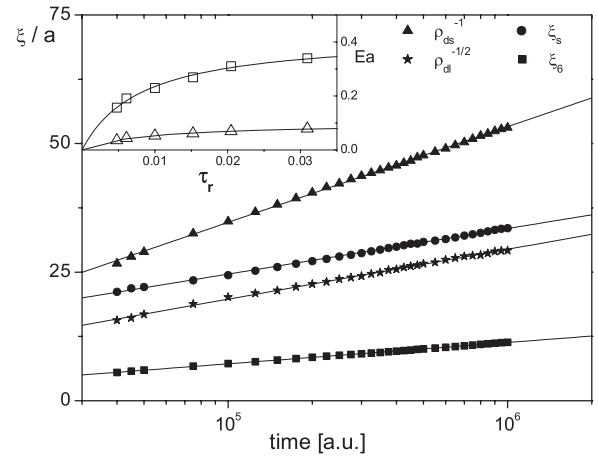

FIG. 2. Time evolution of the different correlation lengths analyzed in this work for $\tau_r = 0.01$ (symbols indicated in the figure) and logarithmic fit (lines). Inset: Activation energy density as a function of τ_r for ξ_6 (squares) and ξ_{ds} (triangles).

certain number of TP remain pinned to their positions (squares).

Since the free energy associated to the hexagonal pattern is invariant under rigid rotations, the bulk energies of the different grains are thermodynamically equivalent. Then the relaxation towards equilibrium is led by the relaxation of the surface energy. This process is responsible for the straightening of the grain boundaries observed in Figs. 1 and 3. Note the similarities of our patterns with the scheme of relaxation proposed by Lifshitz [8] (bottom of Fig. 3). As a consequence of the minimization of the surface energy, the configuration of the grain boundaries radiating from TP acquires well-defined angles. Then these points are feasible to become pinned to their positions once this optimal configuration of the dislocation lines is attained.

Dislocations located along grain boundaries recombine and annihilate each other in order to reduce the curvature. Once the grain has relaxed its curvature, further grain boundary motion requires one to overcome the free energy barriers imposed by the TP and the anisotropy in the line tension. These immobile TP may become activated at larger time scales by a hierarchical process involving the annihilation of a neighbor TP. Once these annihilation events have been accomplished, the activation is started when the lines of dislocation radiating from the TP acquire a configuration where there is an imbalance in the net force acting on the TP.

The pinning of TP leads to the formation of regions trapped into a metastable state, slowing down the process of coarsening. Although this metastable state does not minimize the total free energy of the system, it can be kinetically stable [8].

In addition to the logarithmic dependence of the correlation lengths in time, we have observed that under small perturbations the domain walls involved in equilibrated TP repel each other, in agreement with the theoretical predictions of Safran [9].
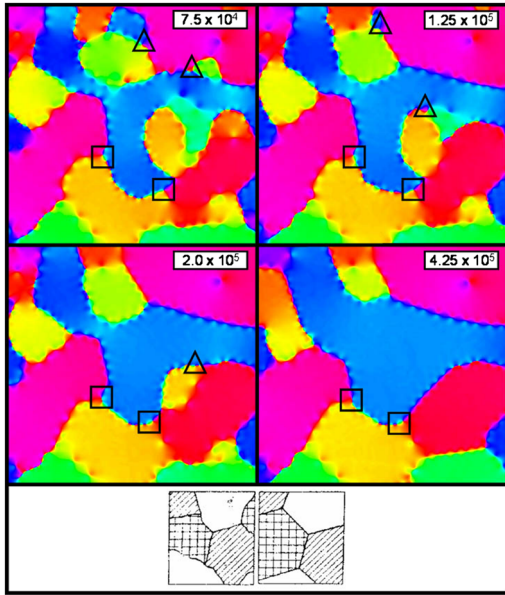
FIG. 3 (color online). Mechanism of coarsening analyzed through orientational maps. Triangles and squares indicate activated and inactivated TP, respectively. Bottom: Formation of a kinetically stable lattice of domains as proposed by Lifshitz.

If some energy barrier U_a is involved in the activation of the TP, the rate of change of the correlation length ξ should be $d\xi/dt \sim \exp(-U_a/kT)$. Since the free energy excess is produced mainly by the interfaces, we have $U_a \sim E_a \xi$, where E_a is the free energy density in units of kT. Then, solving for ξ at long times, we have $\xi(t) \sim (1/E_a) \ln t$.

The inset in Fig. 2 shows the dependence of E_a as a function of τ_r for the orientational correlation length ξ_6 and the correlation length obtained through the dislocations ξ_{ds}. In this inset, it is possible to observe that the activation energy density associated to ξ_6 is about a factor of 4 larger than the associated to ξ_{ds}, in agreement with the qualitative observations. We found that these activation energy densities satisfy the hyperbolic relationship $Ea \sim \tau_r/(\tau_0 + \tau_r)$, where τ_0 is a constant.

Differently from atomistic simulations or experiments with hard colloidal particles, in soft crystals the nanodomain can modify its configuration in order to relax the stress field introduced by the defects [17]. Then, in this class of soft materials, the stress-strain fields associated to the topological defects are not expected to be the same as in hard crystalline solids. These effects can be very important, for example, in determining the interplay between dislocations and disclinations in the Kosterlitz-Thouless transition [18]. However, it is important to emphasize that the phenomenology we are studying is quite general and not specifically limited to diblock copolymers [16].

In conclusion, we have analyzed the process of coarsening in a 2D hexagonal system in the absence of thermal fluctuations. We have found a distinctive region of the phase diagram where the TP dominates the dynamics and can lead to the formation of the kinetically stable configu-

rations of domains proposed by Lifshitz. Triple points pinned to local traps can be activated by a hierarchical process involving the motion and subsequent annihilation of neighbor triple points. Differently from other regions of the phase diagram where the dynamic freezes as a consequence of the Pierls-like forces acting on dislocation lines [14], here these forces are surmounted by the line tension. In the neighborhood of the spinodal line, the temporal evolution of the correlation lengths depends logarithmically on time. It is hoped that this Letter will stimulate experimental research in this region of the phase diagram to study the dynamics of TP.

*Electronic address: dvega@criba.edu.ar
[1] A. J. Bray, Adv. Phys. **43**, 357 (1994).
[2] C. Sagui and R. C. Desai, Phys. Rev. E **52**, 2807 (1995).
[3] M. R. Evans, J. Phys. Condens. Matter **14**, 1397 (2002).
[4] C. K. Harrison, D. H. Adamson, Z. Cheng, J. M. Sebastian, S. Sethuraman, D. A. Huse, R. A. Register, and P. M. Chaikin, Science **290**, 1558 (2000).
[5] C. K. Harrison, Z. Cheng, S. Sethuraman, D. A. Huse, P. M. Chaikin, D. A. Vega, J. M. Sebastian, R. A. Register, and D. H. Adamson, Phys. Rev. E **66**, 011706 (2002).
[6] D. A. Vega, C. K. Harrison, D. E. Angelescu, M. L. Trawick, D. A. Huse, P. M. Chaikin, and R. A. Register, Phys. Rev. E **71**, 061803 (2005).
[7] C. K. Harrison, D. E. Angelescu, M. Trawick, Z. Cheng, D. A. Huse, P. M. Chaikin, D. A. Vega, J. M. Sebastian, R. A. Register, and D. H. Adamson, Europhys. Lett. **67**, 800 (2004).
[8] L. M. Lifshitz, Sov. Phys. JETP **15**, 939 (1962).
[9] S. A. Safran, Phys. Rev. Lett. **46**, 1581 (1981).
[10] J. D. Shore, M. Holzer, and J. P. Sethna, Phys. Rev. B **46**, 11 376 (1992).
[11] T. Ohta and K. Kawasaki, Macromolecules **19**, 2621 (1986).
[12] L. Leibler, Macromolecules **13**, 1602 (1980).
[13] J. L. Goveas and S. T. Milner, Macromolecules **30**, 2605 (1997).
[14] D. Boyer and J. Viñals, Phys. Rev. Lett. **89**, 055501 (2002).
[15] A. Travesset, Phys. Rev. B **68**, 115421 (2003).
[16] See EPAPS Document No. E-PRLTAO-97-017645 for two movies depicting the process of coarsening, motion of dislocations, pinning of triple points, and the process of formation of moiré patterns. For more information on EPAPS, see http://www.aip.org/pubservs/epaps.html.
[17] M. R. Hammond, S. W. Sides, G. H. Fredrickson, E. J. Kramer, J. Roukolainen, and S. F. Hahn, Macromolecules **36**, 8712 (2003).
[18] E. J. Kramer, Nature (London) **437**, 824 (2005).